Static Characteristics of Novel Air-cored Linear and Rotary Halbach Permanent Magnet Actuator

*Ping Jin[1], Yue Yuan[1], Shuhua Fang[2], Hui Yang[2], Kang Wang[2]
[1]School of Energy and Electrical Engineering, Hohai University, Nanjing 211100, China
[2]School of Electrical Engineering, Southeast University, Nanjing 210096, China
*Jinping1981@gmail.com

Abstract—This paper investigates the static characteristics of a novel air-cored linear and rotary Halbach permanent magnet actuator. The magnetic field distributions of the actuator are analytically analyzed using the magnetic scalar potential and modified BESSEL functions in the cylindrical coordinate system. The linear electromagnetic force and rotary electromagnetic torque of the actuator are subsequently predicted validated by the three-dimensional finite element method.

***Index Terms*—actuator, electromagnetic torque, magnetic fields**

I. Introduction

With the growing need of special electromagnetic actuators performing complex movements, linear and rotary actuator capable of linear, rotary and helical movements is of great interest in industrial and domestic products as diverse as robotics and automated manual transmission.

At present, such actuator is realized almost exclusively by using a separate motor/actuator in each moving direction, which results in more complicated structure and heavier mover. Besides, the dynamic performance and servo-tracking accuracy of the actuator are also inevitably compromised due to the effects of inertia, backlash, nonlinear friction, and elastic deformation of gears [1]-[2]. As an advantage design, iron-cored linear and rotary permanent magnet actuator (LRPMA) with high dynamic performance, good power/mass ratio and simple structure has been proposed and analyzed by the finite element method (FEM) [3]-[4] and analytical method [5] in recent years. However, their performances are serious impacted by linear cogging force and rotary cogging torque [6].

This paper presents a novel air-cored LRPMA with a Halbach PM array. The three-dimensional (3D) magnetic field distribution of the LRPMA is formulated by the magnetic scalar potential (MSP) and modified BESSEL functions in a cylindrical co-ordinate system. The electromagnetic torque and electromagnetic force in the rotary and linear directions and the flux linkage of the stator winding are subsequently derived and validated by the 3D FEM.

II. Analytical Analysis of Magnetic Field

A. Air-cored LRPMA with a Halbach PM Array

As shown in Fig. 1, the air-cored LRPMA with a Halbach PM array has a tubular mover, on which there are alternately polarized Halbach PMs, six poles in the z direction and eight poles in the θ direction, and a stator with eighteen coils, three ones in the z direction and six ones in the θ direction.

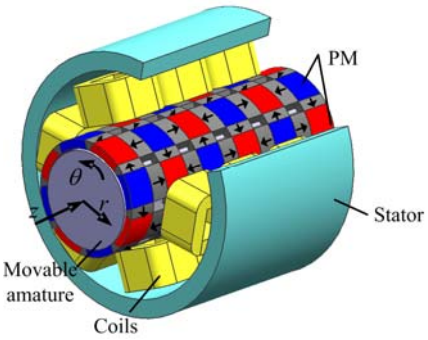

Fig. 1. 3-D cutaway view of air-cored LRPMA with Halbach PM array

Fig. 2 shows the cutaways of the air-cored actuator along the linear and rotational directions. Region I ($R_m \le r \le R_s$) is air/winding region and region II ($R_r \le r \le R_m$) is the PM region. In the 3-D model, the soft-magnetic parts are considered to be infinitely permeable, and the boundaries where $r = R_s$ and $r = R_r$ are of the Neumann boundary; the end effects are not taken into account; the PMs have a linear demagnetization characteristic, and are fully magnetized in the direction of magnetization.

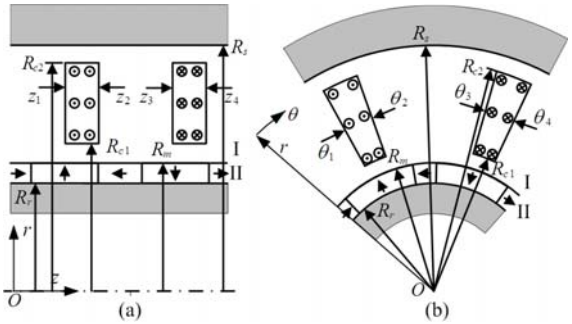

Fig. 2. Cutaways of the LRPMA along (a) axial direction, (b) circumferential direction.

B. Field distribution in Cartesian coordinate system

By solving Laplacian equation in region I and the Possion equation in region II subject to the distributions of magnetization component M_r in the PM region and the boundary conditions, the Fourier expansion of r, θ and z directions flux density components in airgap region I in the 3-D cylindrical coordinate system are given by

$$B_{1r}(r,\theta,z) = -\mu_0 \upsilon \sum_{k=1,3,5\cdots}^{\infty} \sum_{n=1,3,5\cdots}^{\infty} [\frac{IK_8}{IK_3}\cos(v\theta)\cos(\upsilon z) \quad (\frac{H_1 \cdot IK_2 \cdot IK_4}{IK_5 \cdot IK_1} - \frac{H_2 \cdot IK_2 \cdot IK_3}{IK_5 \cdot IK_1} + \frac{H_3 \cdot IK_3 \cdot IK_6}{IK_7 \cdot IK_1} + H_1)] \quad (1)$$

$$B_{1\theta}(r,\theta,z) = \mu_0 v \sum_{k=1,3,5\cdots}^{\infty} \sum_{n=1,3,5\cdots}^{\infty} [\frac{IK_9}{IK_3}\sin(v\theta)\cos(\upsilon z) \quad (\frac{H_1 \cdot IK_2 \cdot IK_4}{IK_5 \cdot IK_1} - \frac{H_2 \cdot IK_2 \cdot IK_3}{IK_5 \cdot IK_1} + \frac{H_3 \cdot IK_3 \cdot IK_6}{IK_7 \cdot IK_1} + H_1)] \quad (2)$$

$$B_{1z}(r,\theta,z) = \mu_0 \upsilon \sum_{k=1,3,5\cdots}^{\infty} \sum_{n=1,3,5\cdots}^{\infty} [\frac{IK_9}{IK_3}\cos(v\theta)\sin(\upsilon z) \quad (\frac{H_1 \cdot IK_2 \cdot IK_4}{IK_5 \cdot IK_1} - \frac{H_2 \cdot IK_2 \cdot IK_3}{IK_5 \cdot IK_1} + \frac{H_3 \cdot IK_3 \cdot IK_6}{IK_7 \cdot IK_1} + H_1)] \quad (3)$$

where $v = np$ and $\upsilon = k\pi/\tau$;

$IK_1 = I_v(\upsilon R_o)K_v(\upsilon R_s) - I_v(\upsilon R_s)K_v(\upsilon R_o)$;

$IK_2 = I_v(\upsilon R_m)K_v(\upsilon R_o) - I_v(\upsilon R_o)K_v(\upsilon R_m)$;

$IK_3 = I_v(\upsilon R_m)K_v(\upsilon R_s) - I_v(\upsilon R_s)K_v(\upsilon R_m)$;

$IK_4 = I'_v(\upsilon R_m)K_v(\upsilon R_s) - I_v(\upsilon R_s)K'_v(\upsilon R_m)$;

$IK_5 = I'_v(\upsilon R_m)K_v(\upsilon R_m) - I_v(\upsilon R_m)K'_v(\upsilon R_m)$;

$IK_6 = I_v(\upsilon R_r)K_v(\upsilon R_o) - I_v(\upsilon R_o)K_v(\upsilon R_r)$;

$IK_7 = I'_v(\upsilon R_r)K_v(\upsilon R_r) - I_v(\upsilon R_r)K'_v(\upsilon R_r)$;

$IK_8 = I'_v(\upsilon r)K_v(\upsilon R_s) - I_v(\upsilon R_s)K'_v(\upsilon r)$;

$IK_9 = I_v(\upsilon r)K_v(\upsilon R_s) - I_v(\upsilon R_s)K_v(\upsilon r)$;

$I_v(\upsilon r)$ and $K_v(\upsilon R_s)$ are the modified BESSEL functions of first and second kind

$$I_v(\upsilon r) = (\frac{k\pi}{2\tau}r)^{\frac{npk\pi}{\tau}} \sum_{k=0}^{\infty} \frac{1}{k!} \frac{1}{\Gamma(k + \frac{npk\pi}{\tau} + 1)} (\frac{k\pi}{2\tau}r)^{2k}$$

and $K_v(\upsilon r) = \lim_{a \to v} \frac{\pi}{2} \frac{I_{-a}(\upsilon r) - I_a(\upsilon r)}{\sin a\pi}$

$I'_v(\upsilon r)$ and $K'_v(\upsilon R_s)$, which are the derivative of $I_v(\upsilon r)$ and $K_v(\upsilon R_s)$, are expressed approximately by

$$I'_v(\upsilon r) = I_{v-1}(\upsilon r) - \frac{v}{\upsilon r} I_v(\upsilon r) \text{ and}$$

$$K'_v(\upsilon r) = -K_{v-1}(\upsilon r) - \frac{v}{\upsilon r} K_v(\upsilon r).$$

$H_1 = \varphi^*_{nk}(\upsilon R_m)$, $H_2 = (\varphi^*_{nk})'(\upsilon R_m) + M_{rnk}/(\upsilon \mu_r)$,

$H_3 = M_{rnk}/(\upsilon \mu_r)$;

where

$$\varphi^*_{nk}(\upsilon R_m) = I_v(\upsilon R_m)\int_{R_r}^{R_m} M_{rnk}K_v(\upsilon\gamma)d\gamma - k_v(\upsilon R_m)\int_{R_r}^{R_m} M_{rnk}I_v(\upsilon\gamma)d\gamma$$

$$(\varphi^*_{nk}(\upsilon R_m))' = I'_v(\upsilon R_m)\int_{R_r}^{R_m} M_{rnk}K_v(\upsilon\gamma)d\gamma - k'_v(\upsilon R_m)\int_{R_r}^{R_m} M_{rnk}I_v(\upsilon\gamma)d\gamma$$

III. Electromagnetic Force and Torque

By neglecting high order harmonic, the electromagnetic force and torque exerted on the rotor can be written as

$$T = T_m(\int_{\theta_1}^{\theta_2} - \int_{\theta_3}^{\theta_4})\sin(p\theta)\cos(\omega_\theta t + \varphi_\theta)d\theta \int_{\vartheta_2}^{\vartheta_3}\cos(\vartheta)\cos(\omega_z t + \varphi_z)d\vartheta \quad (4)$$

$$F = F_m\int_{\theta_2}^{\theta_3}\sin(p\theta)\cos(\omega_\theta t + \varphi_\theta)d\theta (\int_{\vartheta_1}^{\vartheta_2} - \int_{\vartheta_3}^{\vartheta_4})\cos(\vartheta)\cos(\omega_z t + \varphi_z)d\vartheta \quad (5)$$

where $\vartheta = \pi z/\tau$; T_m and F_m, respectively the amplitude of linear electromagnetic force and rotary electromagnetic torque.

Calculations and experiments are performed when windings are excited by ac currents. Fig. 4 shows the results' comparison of the linear electromagnetic force and rotary electromagnetic torque by 3-D analytical prediction and FEM calculation. The results are in good agreement.

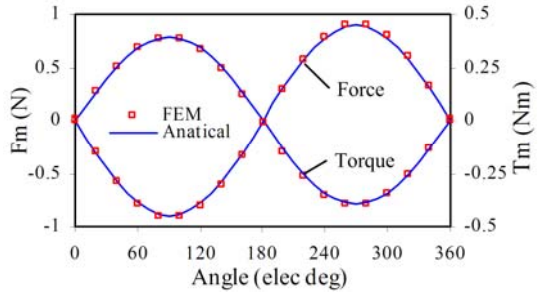

Fig. 4. Results' comparison of the linear electromagnetic force and rotary electromagnetic torque by 3D analytical prediction and FEM calculating.

IV. Conclusions

In this paper, static characteristics of a novel air-cored linear and rotary Halbach permanent magnet actuator has been researched. Based on the magnetic scalar potential and modified BESSEL functions in the cylindrical coordinate system, the 3-D analytical magnetic field distribution and linear electromagnetic force as well as rotary electromagnetic torque of the LRPMA are derived in closed forms and verified by FEM.

References

[1] Bolognesi, O. Bruno, and L. Taponecco, "Dual-function wheel drives using rotary-linear actuators in electric and hybrid vehicles," *in Proc. 35th IECON Conf.*, Porto, Portugal, Nov. 2009, pp. 3916-3921.

[2] E. A. Mendrela and E. Gierczak, "Double-winding rotary-linear induction motor," *IEEE Trans. Energy Convers*., vol. EC-2, no. 1, pp. 47-54, Mar. 1987.

[3] G. Krebs, A. Tounzi, B. Pauwels, D. Willemot, and M. F. Piriou, "Design of a permanent magnet actuator for linear and rotary movements," *European Phys. J.: Appl. Phys*., vol. 44, pp. 77-85, 2008.

[4] G. Krebs, A. Tounzi, B. Pauwels, D. Willemot, and F. Piriou, "Modeling of a linear and rotary permanent magnet actuator," *IEEE Trans. Magn*., vol. 44, no. 11, pp. 4357-4360, Nov. 2008.

[5] P. Jin, S. H. Fang, H. Y. Lin, Z. Q. Zhu, Y. K. Huang, and X. B. Wang, "Analytical magnetic field analysis and prediction of cogging force and torque of a linear and rotary," *IEEE Trans. Magn.*, vol. 47, no. 10, pp. 3004-3007, Oct. 2011.

[6] P. Jin, H. Y. Lin, S. H. Fang, and S. L. Ho "Decoupling control of linear and rotary permanent magnet actuator using two-directional d-q transformation ," *IEEE Trans. Magn.*, vol. 48, no. 10, pp. 2585-2591, Oct. 2012.